Nanotechnology Perceptions
ISSN 1660-6795
www.nano-ntp.com

Influence of Homo Valant (Sr3+) substitution on Dielectric and Conductive Response of BiFeO3 solid solutions

Pankaj Kumar

Department of Physics, RR BAWA DAV College, Batala, Punjab, India
Email: pguptahp78@gmail.com

Trivalent metal ion (Sr3+) modified BiFeO3 nano ceramic solid solutions (BiFeO3 (Bi1-xSrxFeO3, x = 0.1 & 0.5) at Different Temperature) have been synthesized using solid solutions. Prepared solid solution particles have been characterized for dielectric, impedance (electrical modulus) and conductivity response. Effect of temperature on dielectric, impedance (electrical modulus) and conductive behavior in frequency range varied from 100 Hz to 1000 kHz have been analyzed and reported. The thermally activation of dipoles responsible for hopping mechanism to tailored dielectric and impedance response have been analyzed. The effect of temperature results in creation of oxygen vacancies led improvement in conductivity has been recorded and reported. The increment in conductivity has also be confirmed from decrease in resistive response of prepared ceramic solid solutions. The maxima in imaginary part of impedance and electrical modulus evident for appearance of relaxation phenomenon. The shift in maxima with varying frequency towards higher frequency responsible for presence of frequency dependent dielectric relaxation in divalent substituted at Sr3+ in BiFeO3 solid solutions. The conductivity behavior has been analyzed using universal power law $\sigma_{ac}(\omega) = \sigma_{dc}(\omega) + A\omega^n$, where ω is frequency of applied signal of ac field, and n = exponent.

Keywords: Perovskites, Dielectric Relaxation, Space Charge Polarization, Conductivity, Perovskite

1. Introduction

ABO_3 commonly called Perovskite materials become important in last few decades due their distinctive crystal structure (ABO_3 have garnered significant attention in various fields of materials science and engineering due to their exceptional electronic, optical and physical stability. Originally studied for their intriguing ferroelectric characteristics, perovskites have evolved to play a crucial role in modern technological applications, particularly as conducting and dielectric materials. Perovskites exhibit a wide range of tunable properties depending on their composition, making them versatile candidates for both conducting and dielectric functionalities. As conducting materials, certain perovskites, especially transition metal oxides, demonstrate high electrical conductivity, primarily due to the mobile charge carriers generated by their mixed valence states. These conducting perovskites have found applications in solid oxide fuel cells (SOFCs), thermoelectric devices, and electrodes in capacitors and batteries. The diversity in the electronic behavior of perovskites is largely due to the variability in their elemental composition, which allows for engineering materials with specific properties tailored for a wide range of applications. For instance, hybrid organic-inorganic perovskites have emerged as highly promising materials for solar cells, exhibiting both dielectric and semiconducting properties. On the other hand, perovskites are also widely explored as dielectric materials due to their high dielectric constants and tunable polarizability. Their ability to store and dissipate electric energy makes them suitable for applications in capacitors, energy storage systems, and microwave communication technologies. The combination of ionic displacement and the presence of polarizable ions in perovskite structures contributes to their impressive dielectric properties [1-10].

Bismuth ferrite ($BiFeO_3$, or BFO) is a multifunctional perovskite oxide that has attracted substantial interest due to its remarkable coupling of magnetic and dielectric (ferroelectric) properties. As one of the most extensively studied multiferroic materials, $BiFeO_3$ exhibits simultaneous ferroelectricity and antiferromagnetism at room temperature, making it a candidate for numerous applications in spintronics, sensors, and memory devices. $BiFeO_3$ is a canted antiferromagnet, meaning that while its magnetic structure is largely antiferromagnetic (where adjacent magnetic moments are aligned in opposite directions), a small canting of the spins leads to a net weak ferromagnetic moment. This weak ferromagnetism stems from the Dzyaloshinskii-Moriya interaction, a relativistic effect that twists the spin structure in such a way that an overall magnetization is present. The Neel temperature of $BiFeO_3$, above which the material loses its antiferromagnetic order, is relatively high (around 643 K), making it suitable for use in magnetic applications at room temperature. $BiFeO_3$ is a well-known ferroelectric material with a high Curie temperature (approximately 1103 K), which enables it to maintain ferroelectric properties well above room temperature. Its spontaneous polarization along the [111] direction of the rhombohedral crystal structure can be as high as 90-100 $\mu C/cm^2$, which is significantly larger than many other ferroelectric materials. This makes $BiFeO_3$ highly suitable for applications in non-volatile memory devices, such as ferroelectric random-access memory (Fe-RAM). However, challenges remain in the practical deployment of $BiFeO_3$. One of the primary concerns is the high leakage current observed in thin films of $BiFeO_3$, which can degrade its ferroelectric and dielectric properties. Moreover, the material's complex domain structure and the difficulty in achieving high-quality thin films with minimal defects can impact its performance. Researchers are actively investigating methods such as chemical doping, strain engineering, and the fabrication of nanostructures to overcome these limitations [11-19].

In the present work, we have studied the effect of Sr^{3+} substitution on electrical properties of $BiFeO_3$ ($BiFeO_3$ ($Bi_{1-x}Sr_xFeO_3$, x = 0.1 & 0.5) at Different Temperature) synthesized using solid solution was prepared by conventional solid state reaction route. The impedance spectroscopy is a one of very useful & important tool used to explain dielectric relaxation, conductivity response as function of frequency and temperature. The Jonsher's power law of ac conductivity at different temperature explains the hopping mechanism.

2. Experimental Methodology:

Ceramics solid solutions of Trivalent metal ion (Sr^{3+}) substituted $BiFeO_3$ Nano-ceramic solid solutions ($BiFeO_3$ ($Bi_{1-x}Sr_xFeO_3$, x = 0.1 & 0.5)) have been synthesized using solid solutions. Effect of valance state difference on dielectric and conductivity of prepared solid solutions have been characterized and reported. The homo valence state difference of parent & substituted Metal ion (Sr^{3+} & Bi^{3+}) led creation of oxygen vacancies which responsible for increase in conductivity of prepared solid solutions. The various metal ions required as per stoichiometric formula mentioned above weighed in required proportion. All weighed metal ion ions mixed first using motor pestle and then transferred in bottles contains zirconia ball and mixed thoroughly using milling machine. The milling process has been carried out for 12 hours. After completion of milling process, mixed powder taken out from bottles and left for drying. The dried powder calcined at ~1000 °C for 12 hours for phase formation. The calcined powder mixed with 2% wt polyvinyl alcohol (PVA) as binder and pressed into circular disc of ~ 12 mm (diameter) & ~ 1mm thick and sintered at 1200 °C for 2 hours for densifications. Sintered pellets have been characterized for various electric properties such as dielectric, impedance (Electrical modulus) as well as conductive behavior. For this, a conducting electrode has been deposited on circular disc for electric properties measurements. Impedance Spectroscopy becomes one of most commonly used to analyze prepared multiferroic perovskites solid solutions used for capacitive applications.

Complex Impedance Spectroscopy

Complex Impedance Spectroscopy (CIS) is a very useful and significant characterizing technique in material science to study different electrical properties, such as real and imaginary parts of electrical impedance, real and imaginary parts of dielectric permittivity, contribution of grain and grain boundaries in electrical properties by studying Nyquist plots, and conduction mechanism from universal johncher's power fitting of conductivity data at various temperatures. For this, Z vs. θ at different temperatures have been recorded using impedance analyzer E4990A from KEYSIGHT TECHNOLOGIES, India and furnace from JUPITER ENGNEERING WORKS NEW DELHI interfaced with each other. The other parameters such as Z', ε', and Z'', ε'' & σ_{ac} etc. have been calculated from Z & θ using standard formulae.

The impedance analyzer (E4990A) from Keysight Technologies was used to determine these electrical characteristics. Using established equations, all of these parameters were computed from empirically acquired Z versus. θ at different temperatures

$$\text{Complex electric modulus, } M^* = M' + jM''$$

$$\text{Also, } \tan\delta = \frac{\varepsilon''}{\varepsilon'}$$

Where Z', ε', M' and Z'', ε'', M'' denote the real and imaginary parts of the impedance, dielectric constant and electric modulus respectively and j = $\sqrt{(-1)}$. Studying the conduction process using Jonscher's power law [14];

$$\sigma_{ac} = \sigma_{dc} + A\omega^n$$

Where "n" is a dimensionless parameter that provides information on the interaction between mobile ions and the lattice in which they interact, "ac" stands for "ac conductivity," "dc" for "dc conductivity," "A" stands for the dispersion parameter expressing the strength of Polarizability, and so on. Dielectric relaxation is indicated by the maxima in Z" & M" vs. Frequency.

3. Results and Discussion:

Figure 1 shows variation of real part of dielectric permittivity (ε') with temperature. Figure 1 reveals ε' vs. Frequency (KHz) of $BiFeO_3$ ($Bi_{1-x}Sr_xFeO_3$, x = 0.1 & 0.5) at Different Temperature at selected temperature to study response of real part of dielectric permittivity with increasing temperature (K) above room temperature. It has been clearly visualized from graphs that value of real part of dielectric permittivity constantly varies with frequency. At low frequencies, dielectrics respond to externally signal of ac applied electric field by allowing dipoles within material to align, leading to a higher dielectric constant. As frequency increases, the ability of the dipoles to realign decreases results in reduction in value of real part of dielectric permittivity. Eventually, at very high frequencies, only electronic polarization dominates but cannot keep up with the alternating field, resulting in a decrease in the dielectric constant. At low frequencies, molecular dipoles can orient themselves with the electric field, but at high frequencies, their orientation cannot keep up with the rapid changes in the field and polarization known as dipolar polarization whereas displacement of charged species within the material can also contribute to dielectric loss, particularly in ionic compounds results in ionic polarization. This involves the displacement of electron clouds within atoms and becomes significant at very high frequencies known as electronic polarization. The dielectric constant starts to decrease due to the lag in dipole alignment. At very high frequencies (MHz to GHz), the dielectric constant may level off or decrease significantly, as the material's polarization mechanisms are predominantly electronic and cannot respond to the rapid changes [21-24]. It has been clearly visualized from graphs as temperature increases continuously, dielectric constant increases consistently with temperature upto certain value of temperature and then decreases after further increases reveals ferroelectric transition. It has been clearly seen in graphs given below that real part of dielectric permittivity first continuously increases as temperature increases up to certain value of temperature and then starts decreases with further increase in temperature. The increase in real part of dielectric permittivity may results due to achievable energy of thermal barrier of dipoles received from temperature received from external sources. This frequency dependence is crucial when selecting materials for applications like capacitors, insulation, RF components, and communication devices. This temperature after which dielectric transition happen considered to be very crucial because at this temperature, prepared ceramic samples exhibits maximum value of real part of dielectric permittivity.

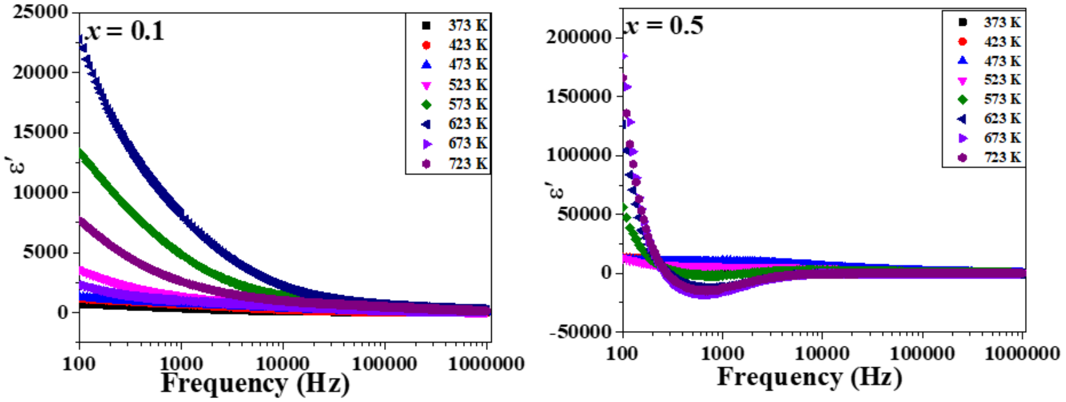

Figure 1: Real Part of Dielectric Permittivity (ε') vs. Frequency (Hz) of Sr^{3+} modified $BiFeO_3$ ($Bi_{1-x}Sr_xFeO_3$, x = 0.1 & 0.5) at Different Temperature

Figure 2 shows variation of imaginary part of dielectric permittivity (ε") with temperature. Figure 2 reveals ε" vs. Frequency (MHz) of $BiFeO_3$ ($Bi_{1-x}Sr_xFeO_3$, x = 0.1 & 0.5) at Different Temperature to study response of real part of dielectric permittivity with increasing temperature (K) above room temperature. It has been clearly visualized from graphs value of real part of dielectric permittivity constantly varies with frequency. At low frequencies, dielectrics respond to externally signal of ac applied electric field by allowing dipoles within material to align, leading to a higher dielectric constant. As frequency increases, the ability of the dipoles to realign decreases results in reduction in value of real part of dielectric permittivity. Eventually, at very high frequencies, only electronic polarization dominates but cannot keep up with the alternating field, resulting in a decrease in the dielectric constant. At low frequencies, molecular dipoles can orient themselves with the electric field, but at high frequencies, their orientation cannot keep up with the rapid changes in the field and polarization known as dipolar polarization whereas displacement of charged species within the material can also contribute to dielectric loss, particularly in ionic compounds results in ionic polarization. This involves the displacement of electron clouds within atoms and becomes significant at very high frequencies known as electronic polarization. The dielectric constant starts to decrease due to the lag in dipole alignment. Imaginary part of dielectric permittivity also considered as dielectric Loss: Along with changes in the dielectric constant, dielectric loss (measured by the loss tangent or dissipation factor) often increases with frequency due to energy dissipated as heat. Dielectric loss refers to the energy dissipated as heat in a dielectric material when it is subjected to an alternating electric field. The behavior of dielectric loss with respect to frequency is an important aspect in applications such as capacitors, insulators, and dielectric resonators [25-29]. Dielectric loss arises from various polarization mechanisms in the material, including: dielectric loss is relatively low because dipoles can effectively orient themselves with the alternating field. It has been seen from graphs given below that imaginary part of dielectric first starts increases initially with increasing temperature. The increase in imaginary part of dielectric permittivity may results due to achievable energy of thermal barrier of dipoles received from temperature received from external sources. The dielectric loss may decrease again in some materials due to capacitive effects, where the material behaves more like a capacitor without significant resistive loss.

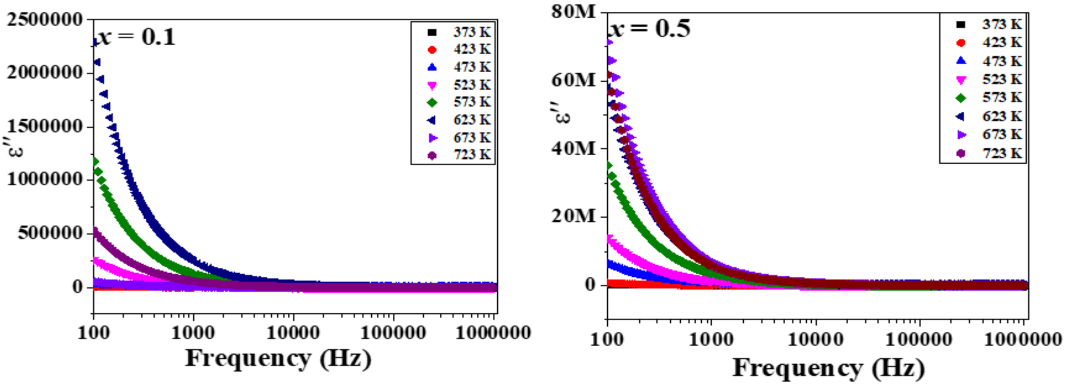

Figure 2: imaginary part of dielectric permittivity (ε") vs. Frequency (Hz) of Sr^{3+} modified $BiFeO_3$ ($Bi_{1-x}Sr_xFeO_3$, x = 0.1 & 0.5) at Different Temperature

Electric modulus is a one of another useful parameter calculated from impedance data helps in describing the dielectric behavior of materials, especially in the context of dielectric relaxation and losses. It provides insight into how charge carriers respond to an electric field and can be helpful for understanding phenomena that lead to energy loss in insulating materials. The electric modulus provides an alternative perspective on the material's electrical characteristics by focusing on how the material responds to an external electric field. As frequency changes, the behavior of the electric modulus can also change significantly. Figure 3 shows real part of Electric modulus (M') vs. Frequency (Hz) of $BiFeO_3$ ($Bi_{1-x}Sr_xFeO_3$, x = 0.1 & 0.5) at Different Temperature at selected temperature. At low frequencies, (M') tends to remain relatively constant. As the frequency increases, (M') may start to rise due to the increasing contributions from charge carrier mobility and polarization effects whereas as frequency increases, (M') can show a peak or continue to increase, reflecting the contribution of different polarization mechanisms (dipolar, ionic, etc.). At high Frequencies, (M') often stabilizes or levels off, indicating that at very high frequencies, the material is dominated more by electronic and less by dipolar/ionic behavior [30-32].

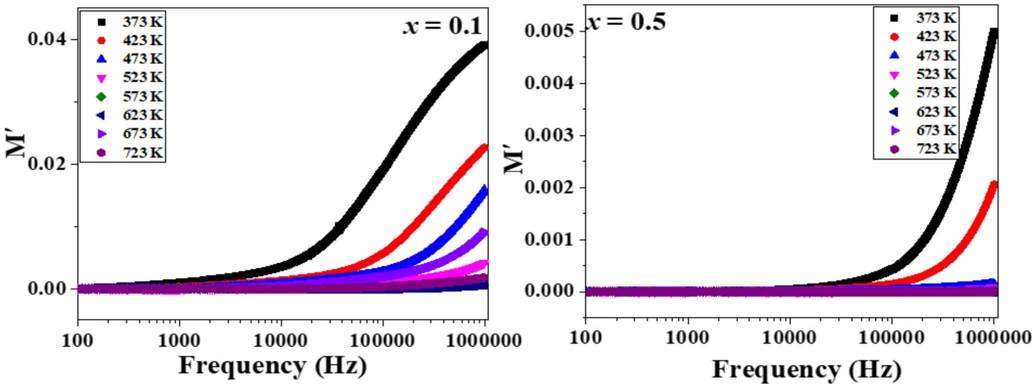

Figure 3: Real part of Electrical Modulus (M') vs. Frequency (Hz) of Sr^{3+} modified $BiFeO_3$

($Bi_{1-x}Sr_xFeO_3$, x = 0.1 & 0.5) at Different Temperature

Figure 4 represent imaginary part of electric modulus (M") vs. Frequency (Hz) of $BiFeO_3$ ($Bi_{1-x}Sr_xFeO_3$, x = 0.1 & 0.5) at Different Temperature at selected temperature. The sharp peaks in M" vs. Frequency reveals presence of dielectric relaxation phenomenon. Relaxation Peaks (M" vs. Frequency) usually correlate with the dielectric relaxation times, indicating the frequencies at which the polarization processes become dissipation-dominant. Variations in the shape, peak position, and height of peaks of M" vs. Frequency profile provide valuable information about the material properties, such as conductivity, dielectric relaxation times, and the types of polarization mechanisms at work. The imaginary part may remain near zero, representing limited dielectric loss. As frequency increases, (M") typically begins to rise sharply. This rise reflects that dipoles and other charge carriers are increasingly unable to orient quickly enough with the alternating electric field. The increased energy dissipation associated with the lagging response of these polarizations leads to a higher (M"), signifying greater dielectric loss. This range is characterized by dielectric relaxation processes, where the imaginary part might peak, representing the frequency at which the maximum energy loss occurs. At very high frequencies, (M") may stabilize or even decrease, depending on the specific material properties [33-35]. This behavior is often attributed to the dominance of electronic polarization mechanisms over slower dipolar and ionic contributions. In this regime, charge carriers can no longer make significant contributions to losses as they cannot respond effectively to the extremely fast changes in the electric field. It has been clearly seen from graphs that as concentration as well as frequency increases, dielectric relaxation starts disappears results increased in conductive response created by homo-valent substitution.

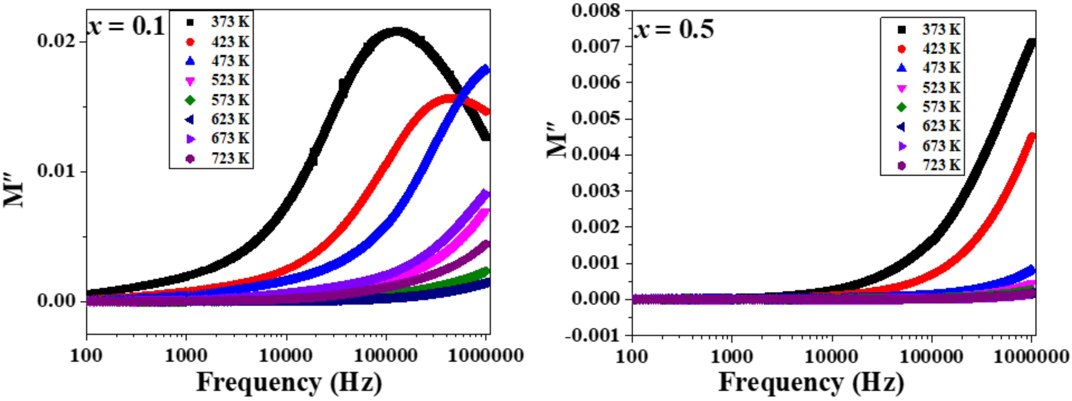

Figure 4: Real part of Electrical Modulus (M") vs. Frequency (Hz) of Sr^{3+} modified $BiFeO_3$ ($Bi_{1-x}Sr_xFeO_3$, x = 0.1 & 0.5) at Different Temperature

Frequency-dependent behavior of as well as influence of temperature on conductivity of Sr^{3+} site on conductive response of $BiFeO_3$ multiferroic perovskites. □$_{ac}$ vs. Frequency (Hz) profile has been used to study change in conductive behavior of $BiFeO_3$ multiferroic perovskite due to Sr^{3+} substitution $BiFeO_3$ ($Bi_{1-x}Sr_xFeO_3$, x = 0.1 & 0.5). ac conductivity □□$_{ac}$) has been calculated from dielectric parameters using formula given below [20-23, 36-37,]

$\sigma_{ac} = 2\pi f \varepsilon' \varepsilon_o \tan\delta$

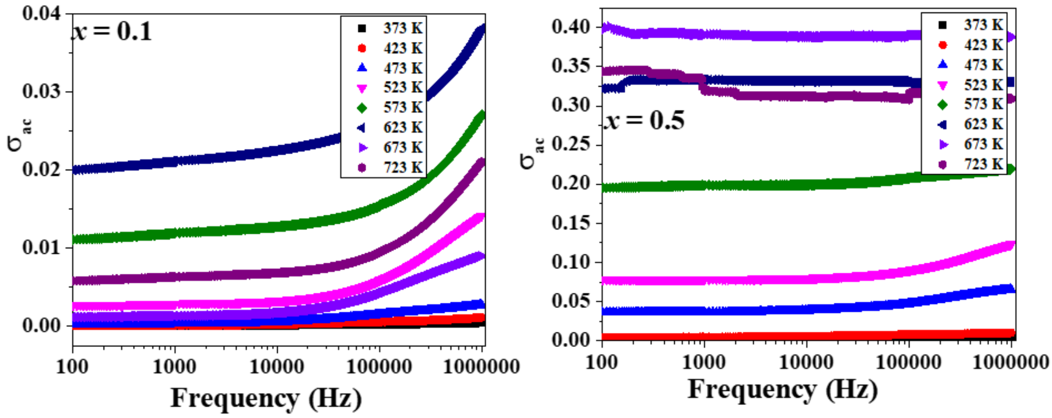

Figure 5: $\square_{ac}$ vs. Frequency (Hz) profile of $BiFeO_3$ ($Bi_{1-x}Sr_xFeO_3$, x = 0.1 & 0.5) at Different Temperature at selected temperature

Figure 5 display $\square_{ac}$ vs. Frequency (Hz) profile of $BiFeO_3$ ($Bi_{1-x}Sr_xFeO_3$, x = 0.1 & 0.5) at Different Temperature at selected temperature. It has been clearly seen in graphs that graphs divided into two parts (a) frequency independence represents to dc conductivity (σ_{dc}) & (b) varied w.r.t. frequency in higher frequency regime termed as ac conductivity (σ_{ac}). The universal johncher's power law has been used to study conduction mechanism from ac conductivity given as follow

$$\sigma_{ac} = \sigma_{dc} + A\omega^n$$

Where σ_{ac} = ac conductivity, σ_{dc} = dc conductivity, A = dispersion parameter representing the strength of Polarizibilty & "n" is dimensionless parameter.

It has been clearly perceived from graphs that conductivity increases with increasing temperature. The increase of oxygen vacancies due to temperature may results for uninterrupted increase in electrical conductivity. [27-29].

4. Conclusion

Trivalent metal ion (Sr^{3+}) substituted $BiFeO_3$ solid solutions ($BiFeO_3$ ($Bi_{1-x}Sr_xFeO_3$, x = 0.1 & 0.5)) have been synthesized using mechanical mixing method. Dielectric permittivity's real as well as imaginary component first rises to a specific temperature before beginning to fall. This indicates that dipoles can receive enough energy from external temperature to react to applied signals easily, while a further decline indicates that dipoles are unable to do so. As the temperature & Sr^{3+} concentration rise, real part of the electrical impedance parameter falls. This is directly related to the electrical conductivity behavior which also get enhanced. The enhancement or increased in value of electric conductivity strongly stamped for increase in concentration of oxygen vacancies. The valance state difference of substituent and parent metal ion and sintering in oxygen deficient environment responsible for increase in concentration of oxygen vacancies.

References

1. V. S. Arunachalam, E. L. Fleischer, Harnessing materials for energy - Introduction. MRS. Bull 33 (2008) 264-276.
2. H. Schmid, Multi-ferroic magnetoelectrics. Ferroelectrics162 (1994) 317-338.
3. T. Zhao, A. Scholl, F. Zavaliche, R. Ramesh, Electrical control of antiferromagnetic domains in multiferroic BiFeO3 film at room temperature. Nature Materials 5, DOI: 10.1038/nmat1731 (2006) 823-829.
4. M. Fiebig, T. Lottermoser, D. Frohlich, A. V. Goltsev, R. V. Pisarev, Observation of coupled magnetic and electric domains. Nature 419, DOI: 10.1038/nature 01077 (2002) 818-820.
5. T. Lottermoser, T. Lonkai, U. Amann, D. Hohlwein, J. Ihringer, M. Fiebig, Magnetic phase control by an electric field. Nature 430, DOI: 10.1038/nature 02728 (2004) 541-544.
6. C. W. Nan, G. Liu, Y. H. Lin, H. D. Chen, Magnetic-field-induced electric polarization in multiferroic nanostructures. Phys. Rev. Lett. 94 (2005) 197203.
7. T. Kimura, T. Goto, H. Shintani, K. Ishizaka, T. Arima, Y. Tokura, Magnetic control of ferroelectric polarization. Nature 426, DOI: 10.1038/nature 02018 (2003) 55-58.
8. W. Eerenstein, N. D. Mathur, J. F. Scott, Multiferroic and magnetoelectric materials. Nature 442 (2006) 759-765.
9. M. Fiebig, Revival of the magnetoelectric effect. Journal of Physics D: Appl. Phys. 38 (2005) R123-R152.
10. M. Bibes, A. Barthelemy, Multiferroics: Towards a magnetoelectric memory. Nature 7 (2008) 425-426.
11. H. Béa, M. Gajek, M. Bibes, A. Barthelemy, Spintronics with multiferroics. Journal of Physics: Condensed Matter 20 (2008) 434221.
12. C. Michel, J. M. Moreau, G.D. Achenbach, R. Gerson, W.J. James, Solid State Commun. 7 (1969) 701.
13. I. Sosnowaska, T. Peterlin-Neumaier, E. Steichele. J. Phys. C 15 (1982) 4835.
14. B. Ruette, S. Zvyagin, A. P. Pyatakov, A. Bush, J.F. Li, V. I. Belotelov, A. K. Zvezdin, D. Viehland, Phys. Rev. B 69 (2004) 064114.
15. T. J. Park, G. C. Papaefthymiou, Athur J. Viescas, A. R. Moodenbaught, S. S. Wong, Nano Lett. 7 (2007) 766.
16. A. Singh, V. Pandey, R. K. Kotnala, D. Pandey, Phys. Rev. Lett. 101 (2008) 247602.
17. M. Kumar, S. Shankar, O. P. Thakur, Anup K. Ghosh, J Mater. Sci: Mater Electron 26 (2015) 1427–1434.
18. A. Singh, C. Moriyoshi, Y. Kuroiwa, D. Pandey, Evidence for local monoclinic structure, polarization rotation, and morphotropic phase transition in (1-x) BiFeO3-xBaTiO3 solid solution: A high-energy synchrotron x-ray powder diffraction study. Physical Review B 88 (2013) 0241113.
19. S.C. Roy, G.L. Sharma, M.C. Bhatnagar, Large blue shift in optical band-gap of sol-gel derived Ba0.5Sr.0.5TiO3 thin films. Solid State Commun. , 141,5 (2007) 243-247.
20. Kumar M, Yadav KL. J. Phys.: Condens. Matter. 2002;19:242202.
21. Cole KS, Robert H. Dispersion and Absorption in Dielectrics:- Alternating Current Characteristics. Journal of Chemical Physics. 1941;9:341–351.
22. Badapanda, T., Sarangi, S., Behera, B., Anwar, S. (2014). Structural and Impedance spectroscopy study of Samarium modified Zirconium Titanate ceramic prepared by mechanochemical route. Current Applied Physics, 14: 1192-1200.
23. Dash, U., Sahoo, S., Chaudhuri, P., Parashar, S.K.S., Parashar, K. (2014). Electrical properties of bulk and nano Li2TiO3 ceramics: A comparative study. Journal of Advanced ceramics. 3: 89-97.
24. Tiwari, B., Choudhary, R.N.P. (2010). Study of Impedance Parameters of Cerium Modified Lead Zirconate Titanate Ceramics. IEEE Transactions on Dielectrics and Electrical Insulation. 17: 5-

17.
25. Badapanda, T., Sarangi, S., Behera, B.,Anwar, S. (2014). Structural and Impedance spectroscopy study of Samarium modified Zirconium Titanate ceramic prepared by mechanochemical route. Current Applied Physics. 14: 1192-1200.
26. Biswal, M.R., Nanda, J., Mishra, N.C., Anwar, S., Mishra, A. (2014). Dielectric and impedance spectroscopic studies of multiferroic BiFe1-xNixO3. Advanced Materials Letter. 5: 531-537.
27. Rajan, R., Kumar, R., Behera, B., Choudhary, R.N.P. (2009). Structural and impedance spectroscopic studies of samarium modified lead zirconate titanate ceramics. Physica B. 404: 3709-3716.
28. Priyanka, Jha, A.K. (2015). Electrical characterization of zirconium substituted barium titanate using complex impedance spectroscopy. Bull. Mater. Sci, 36: 135-141.
29. A. K. Jonscher, Nature 267, 673 (1977).
30. D. K. Pradhan, B. Behera, P. R. Das, J. Mater. Sci. Mater. Electron. 23 (2012) 779.
31. J.C. Dyre, Th.B. Schroder, “Ac hopping conduction at extreme disorder takes place on the percolating cluster”, Phys. Stat. Sol. B, vol. 230 (2002) pp.5.
32. J. M. Le Meins, O.Bohnke, G. Courbion, Ionic conductivity of crystalline and amorphous Na3Al2 (PO4)2F3“, Solid State Ionics, vol.111 (1-2) (1998) 67-75.
33. M.V. Madhava Rao, S. Narender Reddy, A. Sadananda Chary, K. Shahi, “Complex impedance analysis of RbNO3 and RbNO3:Al2O3 dispersed solid electrolyte systems”, Physica B, vol. 364 (2005) pp. 306–310.
34. B. Louati, M. Garouri, K. Guidara, T. Mhiri, “AC electrical properties of the mixed crystal (NH4)3H (SO4)1.42(SeO4)0.58“,J. Phys. Chem. Solids, vol. 66(5) (2005) pp. 762-765.
35. M. Kumar, K. L. Yadav, J. Phys.: Condens. Matter 19 (2002) 242202.
36. S. Havriliak, S. Negami, A complex plane representation of dielectric and mechanical relaxation processes in some polymers. Polymer 8: 161-210. DOI: 10.1016/0032-3861 (1967) 90021-3.
37. T. H. Wang, C. S. Tu, Y. Ding, T. C. Lin, C. S. Ku, W. C. Yang, H. H. Yu, K. T. Wu. Current Applied Physics 11 (2011) S240-S243.